AGE/HMGB1-RAGE axis in systemic sclerosis

Iris Groendijk (s2274191)
Report research internship
Department of Rheumatology and Clinical Immunology
MSc Biomedical Sciences
Supervisor: dr. J. Westra
18th July 2018

Abstract

Introduction. Systemic sclerosis (SSc) is an autoimmune disease characterized by progressive fibrosis of the skin and internal organs, widespread vasculopathy, and autoantibodies against several cellular antigens. An unique feature of SSc is that autoimmunity and vasculopathy precede fibrosis. Microvascular injury results in generation of reactive oxygen species (ROS), which via transforming growth factor-β1 (TGF-β1) causes fibroblast to myofibroblast differentiation and extracellular matrix (ECM) components formation, causing fibrosis in skin and internal organs. Advanced glycation end products (AGEs) are a heterogeneous group of molecules formed under influence of ROS and bind to the receptor for AGEs (RAGE). Also High Mobility Group Box 1 (HMGB1) can bind to RAGE leading to proinflammatory responses. The aim of this study is to investigate the role of the HMGB1/AGE-RAGE axis in the pathogenesis of SSc.

Materials & Methods. Skin biopsies of SSc patients with affected and unaffected skin were stained immunohistochemically for HMGB1, RAGE, AGEs (CML, pentosidine, and MG-H1), and interferon (IFN) type 1 induced protein MxA. Furthermore healthy human dermal fibroblasts (HDFs) were cultured and stimulated with AGE-BSA, HMGB1, and TGF-β1. mRNA levels were measured with RT-qPCR of several parameters including myofibroblast marker α-smooth muscle actin (α-SMA).

Results. MG-H1 expression in SSc skin biopsies is upregulated in both affected and unaffected SSc skin compared to healthy control skin. The other AGEs, HMGB1, and RAGE did not show a clear expression in the SSc skin biopsies. MxA was solely expressed in the epidermis and endothelial cells of SSc skin compared to healthy control skin. After 24 hours of HDF stimulation with different compounds, no difference in α-SMA mRNA expression levels were observed. Interferon induced IFI44L and inflammation related IL-6 were both significantly increased after stimulation with AGE-BSA.

Conclusion. MG-H1 proteins are upregulated in both affected and unaffected SSc skin, indicating it has a role in the pathogenesis of SSc. AGE-BSA stimulation in healthy HDFs did not result in fibrosis, but an inflammatory milieu was created, suggesting a pre-fibrotic stadium.

Table of contents

Introduction

Systemic sclerosis (SSc) is an autoimmune disease characterized by progressive fibrosis of the skin and internal organs, widespread vasculopathy, and autoantibodies against several cellular antigens[1]. Patients who suffer from this disease can have very heterogeneous clinical features[2]. The first symptoms are usually gastro-oesophageal reflux and cold induced discoloration of the skin due to digital artery spasms causing a diminished blood supply know as Raynaud's phenomenon (RP)[3]. SSc has a high mortality rate, predominantly caused by the disease itself. Less commonly, a patients dies because of comorbidities such as infections. The most common cause of death is renal crisis (50%), followed by severe pulmonary arterial hypertension (PAH; 37.5%)[4]. A literature review revealed that the prevalence of SSc is around 50 to 300 cases per million and the incidence varies from 2.3 to 22.8 cases per million per year. The wide range of prevalence and incidence in SSc is due to methodological differences in several studies. In general, women are three times more susceptible to develop SSc compared to men. Also, SSc seems to be more prevalent in Australia and the USA as compared to Europe and Japan[5].

Two clinical subgroups can be divided in the classification of SSc: limited cutaneous (lcSSc) and diffuse cutaneous (dcSSc)[6]. lcSSc is characterised by vascular manifestations. Skin involvement is limited and restricted to the distal parts of the upper and lower extremities, as well as the face. Raynaud's phenomenon is noticed years before the onset of fibrosis. Severe pulmonary hypertension is common, while other organs are often not involved. dcSSc is a rapidly progressive disease with widespread skin involvement, including the proximal parts of the skin. Furthermore, at least one internal organ is compromised, such as large and small intestines involvement, pulmonary fibrosis and/or renal crisis[1,7,8].
In over 95% of the SSc patients, anti-nuclear antibodies (ANAs) are found. SSc-specific ANAs target various nuclear components involved in essential cellular processes, such as cell division, splicing, and transcription. These autoantibodies specific for SSc, because they are rarely associated with other diseases. Therefore ANAs might be usefull as biomarker in clinical practise, especially in dividing SSc patients into the lcSSc and dcSSc subtypes. Two classic SSc-specific ANAs are anticenteromere antibody (ACA) and anti-topoisomerase I antibody (ATA). Whereas in 50-90% of the lcSSc patients ACAs are present, ATAs are predominantly found in dcSSC patients[9].

An unique feature of SSc is that autoimmunity and vasculopathy precede fibrosis. The pathogenesis starts with microvascular injury, which can be caused by many factors like tissue hypoxia, viruses, autoantibodies, defective vasculogenesis or endothelial cell activation. The injury of vascular endothelial cells results in generation of reactive oxygen species (ROS) and activates (a reaction for) vascular remodelling by intravascular coagulation and luminal occlusion, leading to a reduced blood flow and tissue hypoxia. Activated endothelial cells secrete several mediators among which endothelin-1 (ET-1) and transforming growth factor-β1 (TGF-β1) causing vascular smooth muscle cell (VSMC) proliferation and fibroblast activation into myofibroblasts. Hypoxia itself is also a potent trigger for fibroblast activation[10], but the main trigger for fibroblast activation and differentiation into myofibroblasts is TGF-β1[11]. The TGF-β receptor is elevated in SSc fibroblasts, suggesting autocrine TGF-β stimulation of the synthesized cells[12,13]. Myofibroblasts are seen as the key effector cells in fibrosis that deposit the characteristic extracellular matrix (ECM), like collagen I and collagen III and many cytokines and chemokines. As a result, the tissue architecture is replaced by collagens-containing ECM components, leading to tissue stiffening and impaired function[14]. Already in the 1970s, Leroy was the first to demonstrate that SSc skin fibroblasts synthesize increased amounts of collagen *in vitro* compared with healthy control fibroblasts[15,16].

In normal wound healing, damage or injury leads to vascular remodelling and tissue regeneration. The problem in fibrosis is persistent fibroblast activation due to hypoxia, lack of angiogenesis, ROS and

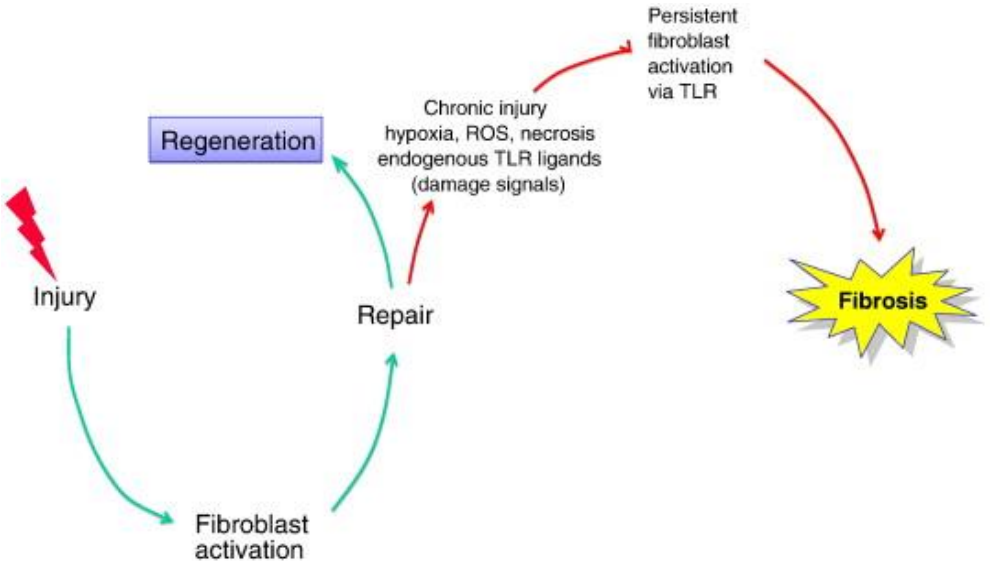

Figure 1. In normal wound healing, the innate immune system has a self-limited repair system. After injury, fibroblasts gets activated leading to a fibrogenic process which completes tissue regeneration. In the case of recurrent or sustained injury, fibroblasts remain activated leading to excessive fibrogenesis via toll like receptor (TLR) activation [17].

persistent TFG-β1 production in a vicious circle manner (*figure 1*). Hereby the ECM stiffening progresses into overt fibrosis[14]. Also, removal of myofibroblasts and endothelial cells through apoptosis is a crucial step in normal wound healing[1,18].

Other compounds related to oxidative stress and vascular damage are advanced glycation end products (AGEs)[19]. AGEs are a heterogeneous group of molecules which are formed under influence of oxidative and glycemic stress[20,21]. This process is also known as the Maillard reaction, named after L.C. Maillard who first described this reaction in 1912. Glycation is a posttranslational modification of the amino groups in proteins, lipids and nucleic acids which reacts non-enzymatically with reducing sugars such as glucose. A series of reactions results in the formation of Schiff bases and Amadori products, which in turn undergo progressive dehydration, cyclization, oxidation, and rearrangement to produce AGEs[19,22]. In contrast to Amadori products, the formation of AGEs is slowly and irreversible leading to accumulation in the body[23]. When oxidation accompanies the glycation process then the products are known as glycoxidation products. Examples hereof are N^{ε}-(1-carboxymethyl)-L-lysine (CML) and pentosidine. Another group of AGEs are reactive intermediate products which are formed during Amadori rearrangement, for example methylgloxal (MG) and 3-deoxyglucosone (3-DG)[22]. These so called dicarbonyl metabolites are important glycation adducts in physiological systems. 90% of the adducts formed is the arginine-derived AGE hydroimidazolone N_{δ}-(5-hydro-5-methyl4-imidazolon-2-yl)-ornithine (MG-H1)[24].

Accumulation of AGEs is found during healthy aging[25], but also in many pathological conditions like diabetes mellitus[23,26], atherosclerosis[19], peripheral artery disease[27], and SSc[28]. The harmful consequence of AGE accumulation is the formation of covalent cross-links. This leads to stiffness of the protein matrix, hence impaired function of organs and vasculature[22].
The receptor for advanced glycation end products (RAGE) is identified by its ability to bind and mediate the effect of AGEs, originally linked to diabetic complications[29]. Relatively recent, Yoshizaki et al were the first to show an overexpression of RAGE in fibrotic skin of SSc patients[30]. RAGE is expressed at several cell types including microvascular endothelial cells, fibroblasts and ECM structures like collagens and elastin[31]. There are conflicting results about whether AGEs are upregulated in SSc, just like in many other autoimmune diseases[32].

RAGE is also a receptor for non-AGE ligands among which High Mobility Group Box 1 (HMGB1). When this nuclear protein gets released into the extracellular space, it can react as a damage-associated molecular pattern (DAMP)[33]. This DAMP has been shown to activate a proinflammatory signalling cascade through its interaction with RAGE and promotes several proinflammatory responses, for example release of inflammatory cytokines like interleukin 6 (IL-6) and tumor necrosis factor α (TNF-α)[29,34,35]. In the context of SSc, not many studies are performed so far, but there are a few studies who associate HMGB1 with SSc[30,36]. Moreover, other studies suggest a role for HMGB1 in the conversion of fibroblasts to myofibroblasts, so there seems to be an influence in the fibrosis process[37,38].

Another group of molecules which are potentially responsible for the immunological damage in SSc patients are type 1 interferons (IFNs). Type 1 IFNs are a heterogeneous family of cytokines, which are initially known for induction of cellular resistance to viral infections. Plasmacytoid dendritic cells (pDCs) are the main producers of type 1 IFNs in reaction to activated TLRs by DAMPs. The increased amounts of type 1 IFNs is reflected by the "interferon-signature", meaning an increased expression of IFN type 1 induced gene expression profile[39,40]. The interferon signature is observed in multiple autoimmune diseases including SSc[41]. A possible link exist between type 1 IFN and fibrosis in SSc patients, although this needs to be further examined.

Collectively, RAGE and its ligands are interesting molecules to study in the pathogenesis of SSc. Therefore, the aim of this study is to investigate the role of the HMGB1/AGE-RAGE axis in the pathogenesis of SSc. First, the localization of several AGEs, HMGB1 and RAGE in skin biopsies of SSc patients with and without affected skin will be investigated. Furthermore, the in vitro influence of AGEs and HMGB1 on human dermal fibroblasts (HDFs) will be examined and whether this leads to an increase of interferon (IFN) type 1 signature, fibroblast to myofibroblast conversion, inflammation, and expression of fibrotic markers.

Materials & Methods

Skin Samples

To evaluate the expression of HMGB1, RAGE, AGEs (CML, pentosidine, and MG-H1), and interferon type 1 induced myxovirus resistance protein 1 (MxA)[42] in the skin, biopsies of 12 SSc patients were stained for these proteins. The biopsies have been taken previously for clinical practice (PALGA database) and are embedded in paraffin. Sections of 4 µm were cut by the pathology department of the Universitary Medical Centre of Groningen (UMCG) and stored at room temperature. All persons have diagnosed SSc according to the 2013 EULAR/ACR clinical criteria[43]. The patients were subdivided into two experimental groups based on the histomorphology of hematoxilin-eosin staining, judged by a skilled pathologist: 6 patients with affected skin and 6 patients with unaffected skin. This samples were compared to the skin of one healthy control. None of the patients are diagnosed with diabetes mellitus.

Immunohistochemistry Skin Biopsies

For immunohistochemistry, the sections were deparaffinised using xylene (2x 10 min), 100% ethanol (2x 5 min), 96% ethanol (2x 5 min), 70% ethanol (2x 5 min) and demi water (1x 5 min). Antigen retrieval was performed at 90^{o}C for 60 min in 10 µM Tris HCl pH 9. Except for HMGB1 and CML, therefore sodiumcitrate buffer pH 6 was used. The sections were blocked for endogenous peroxidase with 0.3% H_2O_2 in phosphate-buffered saline (PBS) to prevent nonspecific binding of antibodies. After washing with PBS the sections were incubated overnight at 4 ^{o}C with the primary antibody: mouse monoclonal anti-CML 1:600 (ab30917; clone NF-1G; Abcam); mouse monoclonal anti-RAGE 1:15000 (MAB5328; lot # PSO1443399; Chemicon); rabbit polyclonal anti-HMGB1 1:800 (ab18256; lot # GR193547-1; Abcam); mouse monoclonal anti-pentosidine 1:300 (orb27502; clone PEN-12; Biorbyt); mouse monoclonal anti-MG-H1 1:10000 (STA-011; lot # 01.4712; Cell Biolabs); and goat polyclonal anti-MxA 0.1 µg/ml and 0.3

µg/ml (AF7946; accession # P20591; R&D). The primary antibodies were diluted in PBS 1% bovine serum albumin (BSA), except from the anti-MxA which was diluted in PBS 1% fetal calf serum (FCS).
After washing with PBS again, the secondary antibodies were added for 1 hour at room temperature polyclonal goat anti-rabbit immunoglobulins/HRP 1:50 (p0448; lot # 20042622; Dako); polyclonal rabbit anti-mouse immunoglobulins/HRP 1:50 (p0260; lot # 20045584; Dako); and rabbit polyclonal anti-goat immunoglobulins/HRP 1:50 (p0449; lot # 20002659; Dako). Also negative controls were stained whereby the primary antibody was replaced for either PBS 1% BSA or PBS 1% FCS. The antibodies were visualized using liquid 3,3'-diaminobenzidine tetrahydrochloride+ (DAB) autostainer (K3468; lot # 10124756; Dako). The sections were counterstained with haematoxylin for 5 seconds.
The immunohistochemistry protocol, as well as the dilution of the antibodies, were carefully established by using sun exposed skin biopsies from healthy controls and SLE patients which were leftovers of a previous study.

Semi-Quantitative Analysis of Staining
The evaluate the expression of HMGB1, RAGE, the AGEs, and MxA, the healthy control tissue sample was judged first and next the SSc samples were scored relative to the healthy control in a semi-quantitative manner: similar expression (/) mild increased expression (+), moderate increased expression (++) strongly increased expression (+++). The total score of one biopsy was scored on the basis of several skin components, namely, the epidermis, adnexes, muscle tissue, endothelial cells, infiltrate and fibroblasts (*figure 2*). This was done for all different antibodies.
The HMGB1 skin biopsies were slightly different judged compared to the AGEs, RAGE, and MxA. HMGB1 is a nuclear protein which can be released either passive or active[33]. It is well visible in the biopsies if HMGB1 is still in the nucleus or if it is released into the cytoplasma. In the healthy control skin, all the nuclei contained HMGB1 and were stained. When some nuclei were out of HMGB1 they were scored +, and when even more nuclei were out of HMGB1 they were scored ++ (*figure 3*). The score +++ was never given.
Each sample was discussed by 5 researches before the final score was given. For statistical analysis and graph formation the semi-quantitative scores were converted to numbers: + to 1, ++ to 2, and +++ to 3.

Cell Culture
HDFs were provided from the department of dermatology of the UMCG. HDFs were grown in DMEM medium (31966-021; lot # 1894785; Gibco by Life Technologies / L0104-500; lot # S17259L0104; Biowest) supplemented with 10% FCS and 1% 10000 U/ml penicillin and 10000 U/ml streptomycin (DE17-602E; lot # 5MB135; Lonza). Cells were incubated at 37 ^{o}C in a humidified atmosphere with 5% CO_2 in 75 cm^2 cell culture flasks (430725U; Corning Incorporated). They were routinely passaged using 3 ml 0.05% trypsin.

Treatment of Cells
HDFs of passage 12-13 were seeded at 300000 cells per well in 6-well plates in 1 ml DMEM containing 10% FCS and 1% penicillin and streptomycin. After 24 hours medium was replaced for starvation medium which contains only 1% FCS. Again 24 hours later, cells were treated with 1, 10, and 100 µg/ml AGE-BSA (121800-10MG; lot # 2952699; Merck), 1, 3, and 10 µg/ml bovine HMGB1 (9050; lot # 150021; Chondrex) and as a positive control for myofibroblast activation, they received 1, 10 and 50 ng/ml (HEK293 derived) human recombinant TGF-β1 (100-21-10UG; lot # 1217209 A1118; Peprotech). To exclude the effect of BSA in the AGE-BSA treatment, some cells were treated cells with 1, 10, and 100 µg/ml BSA. As a negative control, one well was provided with medium without stimulatory agents. The stimulation treatment was done for 24 hours. Afterwards, the HDFs were removed from the plate with TRIzol Reagent (15596018; lot # 16655301; Ambion by Life Technologies) and stored at -80 ^{o}C. At the end of each treatment interval culture supernatants were harvested and stored at -20 ^{o}C. Cell viability was evaluated using a counting chamber (Bürker-Türk) and trypan blue 0.4%.

RNA Isolation and RT-qPCR

RNA was extracted from HDFs using TRIzol Reagent (15596018; lot # 16655301; Ambion by Life Technologies) and were kept at -80 ^{o}C until further use. After isolation, RNA concentrations were quantified with a NanoDrop 1000 spectrometer (Thermo Fisher scientific). The RNA concentration of all samples were equalled at 100 ng/µl, by adding sterile water (Versylene Frensius). Next, 25 µg of each sample was transferred to a small PCR cup. When the initial RNA concentration was below 100 ng/µl, 25 µl was transferred to a PCR cup, without adding anything. Subsequently, samples were heated till 65 degrees for 10 minutes. From there on they were kept on ice. The amount of RNA was equalized in each sample and copyDNA (cDNA) was synthesized by adding a mix (containing 25 mM dNTP's, M-MLV RT enzyme, 5x First Strand buffer, 0.1M DTT, Oligo(dT)12-18 primer and DEPC water) (AM1906; lot # 00493984; Invitrogen by Thermo Fisher Scientific) to the samples and put them in a MyCycler thermal cycler (Bio-Rad). The thermal cycler settings were as followed: first 60 minutes at 41 ^{o}C, than 5 minutes at 95 ^{o}C, and finally they were kept at 16 ^{o}C until the Bio-Rad was turned off manually. The cDNA samples were kept at -20 ^{o}C until further use.

To establish the effect of the fibroblast stimulations on mRNA expression, mRNA expression of α-SMA, RAGE, IL-6, TLR4, TGF-β1, and IFI44L was measured with real time quantitative polymerase chain reaction (RT-qPCR). GAPDH was used as a reference gene. cDNA was added to 384-well plates (Applied Biosystems by Life Technologies) in duplicate/triplate. The DNA samples were dried in the speedvac for 10 minutes at medium drying rate. Afterwards the qPCR probe master mix (BR0500503; Biotechrabbit) was added to the plates and the plates were sealed with an Optical Seal (4311971; Thermo Fisher). The RT-qPCR reaction was performed using Quantstudio 7 Flex (applied biosystems by Life Technologies).

Immunofluorescence Staining of Fibroblasts

To visualize the fibroblast to myofibroblast conversion by HMGB1, AGE-BSA, and TGF-β1 stimulation, fibroblast were cultured in an eight-well glass slide, Lab-tek II Chamber Slide system (154534; lot # 061608 8 6). 1.5 x 10^4 cells per well were cultured in 100 µl medium, stimulated and treated exactly the same way as the fibroblasts suitable for PCR. After 24 hours of stimulation, the cells were washed with PBS, fixed with 1% formaldehyde (244747; Bufa B.V., Pharmaceutical products) for 20 minutes at room temperature, washed three times with PBS, and permeabilised with 0.2% Triton X-100 at room temperature for 30 minutes. Blocking was performed with 2% BSA for 30 minutes at room temperature, followed by incubation with 100 µl/well mouse monoclonal to alpha smooth muscle actin 5 µg/ml (ab7817; lot # GR3190124-3; Abcam), diluted in PBS+ (0.5% Tween, 0.5% BSA in PBS) overnight at 4 °C. After washing three times with PBS+ the cells were incubated with DAPI (10 236 276 001; lot # 70317525; Roche Diagnostics GmbH) in PBS+ 100 µl/well for 15 minutes in the dark, washed again three times with PBS+ and incubated with 100 µl/well goat anti-mouse IgG (H+L)-FITC (1031-02; lot # K6902-XE45; Southern Biotech), and diluted in PBS+ for 30 minutes at room temperature in the dark. Finally, the cells were cover slipped with citifluor glycerol/PBS solution.

Immunohistochemical Staining of Fibroblasts

Again 1.5 x 10^4 cells/well were cultured in an eight-well permanox slide, Lab-tek Chamber slide system (177445; lot # 1024834 2804). Stimulation, fixation, and permeabilization were performed as described above. The cells were incubated overnight with primary antibodies at 4°C: mouse monoclonal to alpha smooth muscle actin 5 µg/ml (ab7817; lot # GR3190124-3; Abcam); mouse monoclonal anti-human fibroblast, clone 5B5 1:50 (M0877; lot # 094(011); Dako); mouse monoclonal fibroblast antibody FITC, clone AS02 1:25 (DIA 120; lot # 0796; Dianova). All antibodies were diluted in PBS 1% BSA. After washing three times with PBS, the secondary antibody was added in 100 µl/well for 30 minutes: polyclonal rabbit anti-mouse immunoglobulins/HRP 1:50 (p0260; lot # 20045584; Dako). Then, the cells were washed again three times in PBS, incubated with DAB autostainer (K3468; lot # 10124756; Dako) for 10 minutes, and counterstained with haematoxylin for 5 seconds. Finally the cells were washed for 10 min under running tap water and were cover slipped with Kaiser's glycerol gelatin (Millipore).

Statistical Analysis

Statistical analysis were performed using GraphPad Prism 5.00 software (GraphPad Software, Inc.). The statistical significance of the skin biopsies was evaluated by an unpaired t-test. The PCR results were evaluated with either an unpaired or a paired t-test. A p value of $p<0.05$ was considered as statistically significant and noted *, $p<0.01$ and $p<0.001$ were indicated by respectively ** and ***.

Results

(R)AGE Expression in SSc Skin Biopsies

Immunohistochemistry showed a really strong expression of RAGE in all components of the skin. Since RAGE is a transmembrane receptor[29], RAGE expression was expected to be solely attached to the cell membrane and the nuclear membrane. The observed expression was considered to be aspecific and we decided to not score this biopsies.

One of the most prominent AGEs in SSc seems to be MG-H1. There is an increased expression in all skin components of SSc skin compared to healthy control skin (*figure 3A*). To compare MG-H1 expression of affected SSc skin with unaffected SSc skin, median expression of all skin components was calculated for each patient. No differences in MG-H1 expression were observed between affected and unaffected SSc skin. However, the expression in both groups is increased compared to the healthy control (*figure 3B*). It is well known sun exposure is of influence on the accumulation of AGEs in the skin[44], so we divided our biopsies into a sun exposed group and a non-exposed group based on the location of the biopsy (*table 1*). One of the biopsies has an unknown location, so this patient was excluded in the sun exposed versus non-exposed comparisons. No differences in MG-H1 expression were observed between the sun exposed and non-exposed groups (*figure 3C*).

Both pentosidine and CML showed a similar expression in SSc skin compared to healthy control skin (data not shown). Remarkable, the CML stained biopsies showed a strong colocalization with elastin fibers in the majority of the patient (*figure 4C*). Even a weak colocalization with elastin fibers was seen in the healthy control (*figure 4A*). Also a strong staining of the stratum corneum was noticed in some the patients (*figure 4B*).

Table 1. Patient characteristics SSc skin biopsies.

	M/F	**Affected skin?**	**Diagnosis SSc**	**Age at biopsy**	**Year of biopsy**	**Location biopsy**	**Sun exposed?**
Patiënt 1	M	Yes	2015	58	2015	coeur and left hand	yes
Patiënt 2	F	Yes	2003	52	2003	groin	no
Patiënt 3	F	Yes	2008	54	2008	upper leg	no
Patiënt 4	F	yes	2001	54	2001	dorsum	yes
Patiënt 5	F	yes	2009	64	2009	lower arm	yes
Patiënt 6	F	yes	2005	57	2005	wrist	yes
Patiënt 7	F	no	2012	61	2012	digitus manus	yes
Patiënt 8	M	no	1999	55	2001	unknown	unknown
Patiënt 9	F	no	2009	50	2006	dorsum	yes
Patiënt 10	M	no	1996	61	2002	upper arm	no
Patiënt 11	F	no	2012	69	2012	digitus manus	yes
Patiënt 12	F	no	2011	37	1997	shoulder	no

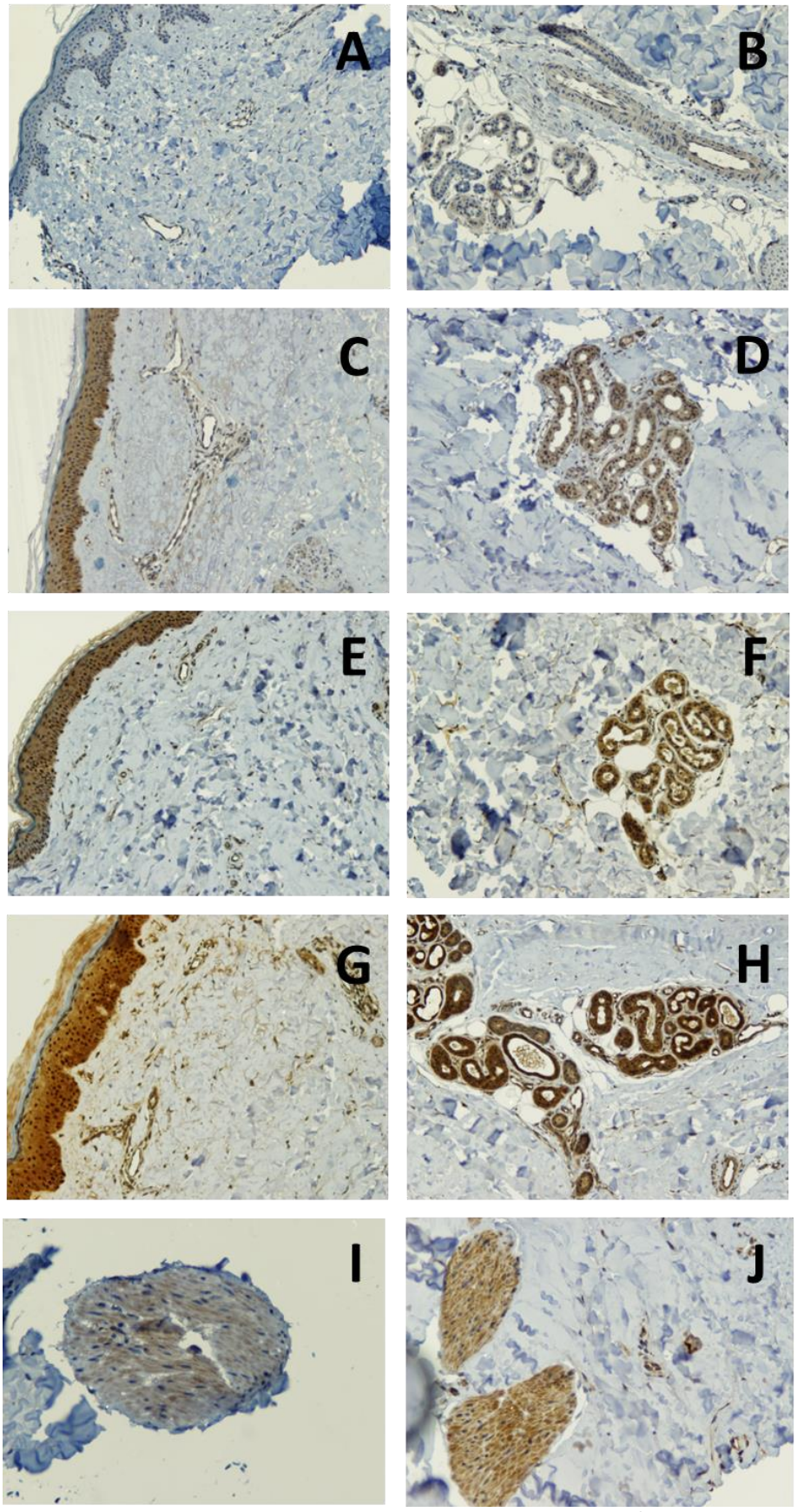

Figure 2. Histological aspects and scoring criteria MG-H1 stained skin biopsies. A, B, I) healthy control. **C-H, J)** systemic sclerosis patient. **C, D)** all skin components scored +. **E)** epidermis scored ++, endothelium and fibroblasts +. **F)** all skin components scored ++. **G)** epidermis scored +++, endothelium, infiltrate and fibroblasts scored ++. **H)** adnexa scored +++. **J)** muscle tissue scored +.

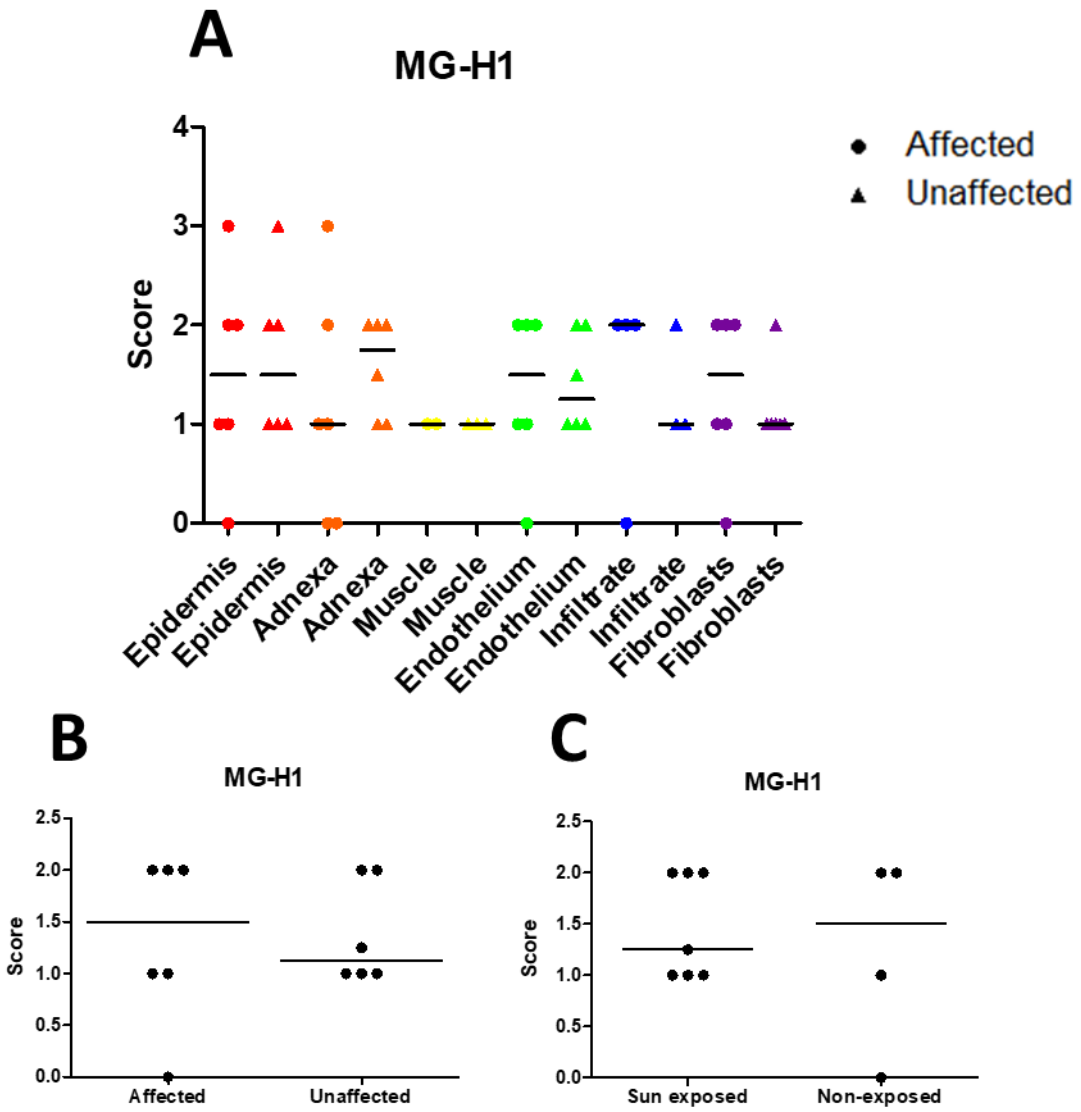

Figure 3. A) MG-H1 expression in different skin components in affected and unaffected skin of systemic sclerosis patients. Line at median. **B)** median score of MG-H1 expression in affected versus unaffected skin of systemic sclerosis patients (n=6). **C)** median score of MG-H1 expression in sun exposed (n=7) versus non-exposed (n=4) skin of systemic sclerosis patients.

HMGB1 Expression in SSc Skin Biopsies

Some SSc biopsies showed increased activation of HMGB1, divided over the different components of the skin compared to the healthy control (*figure 5*). We compared affected SSc skin with unaffected SSc skin and could not find any difference in HMGB1 activation. Also the sun exposed and unexposed groups did not differ from each other (data not shown). For this we calculated again the median score of all skin components of each patient. Remarkable was a strong colocalization with elastin fibers which was visible in almost all biopsies (*figure 5A, 5C*). Also in some biopsies was some staining of the cytoplasm.

MxA expression in SSc skin biopsies

MxA expression in the SSc skin biopsies was solely increased in the epidermis and endothelium (*Figure 6B, C, D*), compared to the healthy control (*figure 6A*). In the other skin structures, no differences were observed (*figure 7A*). For this reason, the final analysis was performed based on solely this two skin structures. The average score was calculated from the epidermis and endothelium of each patient. There seems to be an increased MxA expression in the SSc biopsies compared to the healthy control,

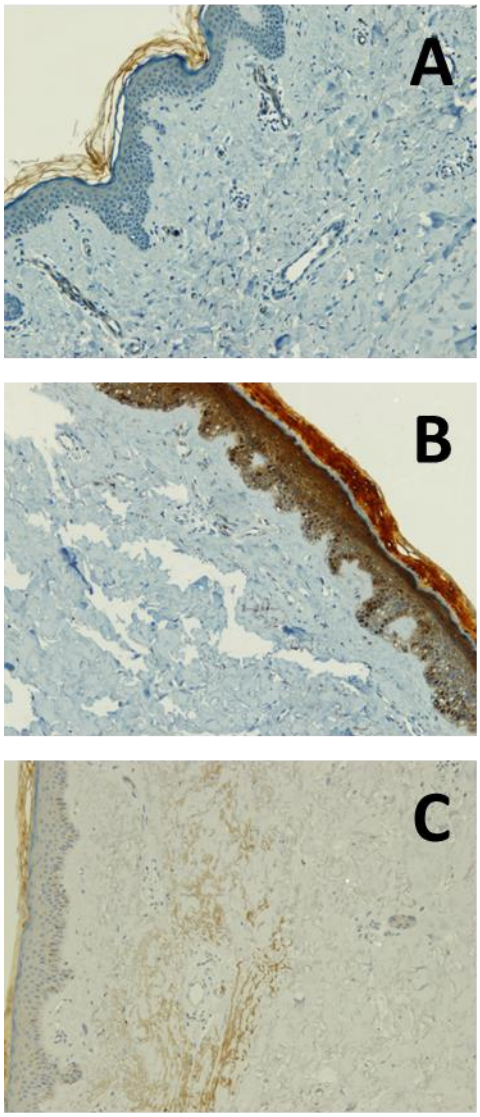

Figure 4. Histological aspects of CML stained skin biopsies. A) healthy control. **B, C)** systemic sclerosis patients. **B)** CML expression on stratum corneum. **C)** colocalization of CML with elastin fibers.

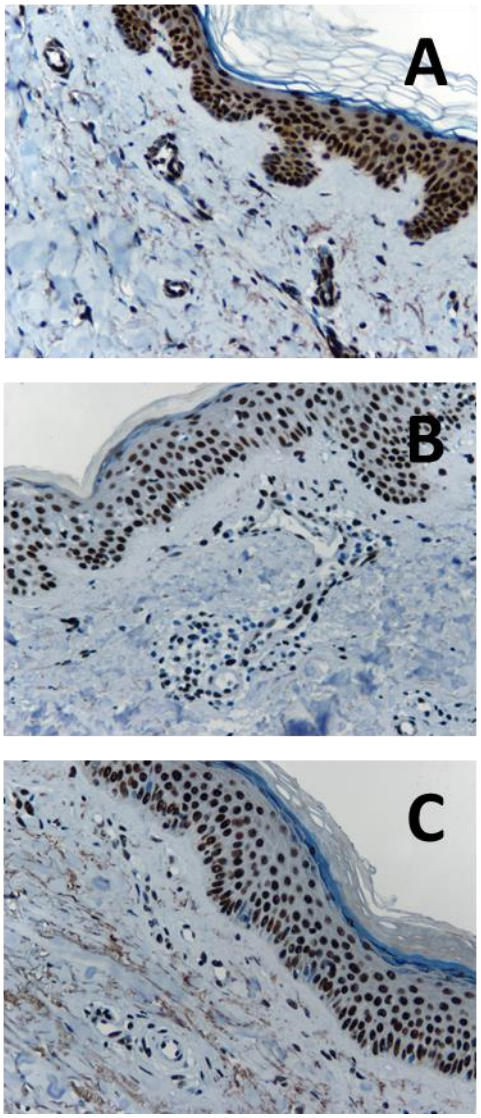

Figure 5. Histological aspects and scoring criteria of HMGB1 stained skin biopsies. A) healthy control. **B, C)** systemic sclerosis patients. **B)** epidermis and endothelium scored +, infiltrate scored ++. **C)** epidermis and infiltrate scored +, colocalization with elastin fibers.

but no significant difference is found between the affected SSc skin and unaffected SSc skin (*figure 7B*). Also no difference was found between sun exposed SSc skin and non-exposed SSc skin (data not shown).

Fibroblast Stimulation

After 24 hours of stimulation with either HMGB1, AGE-BSA or TGF-β1 in several concentration, the myofibroblast marker α-SMA mRNA expression did not increase in the dermal fibroblasts. There even seems to be a decreased expression, but no significant decrease was found (*figure 8A*). Also the expressions of TGF-β1, TLR4 and RAGE did not increase compared to the unstimulated fibroblasts (*figure 8D, E, F*). However, the inflammation marker IL-6 showed a significant increased expression after stimulation with AGE-BSA and a high dose TGF-β1 compared to the unstimulated cells. Even after the low dose TGF-β1 stimulation, IL-6 levels seems to increase, but due to a large error bar this difference is not significant (*figure 8B*). (IFN induced) IFI44L expression was significantly increased after stimulation with AGE-BSA (*figure 8C*).

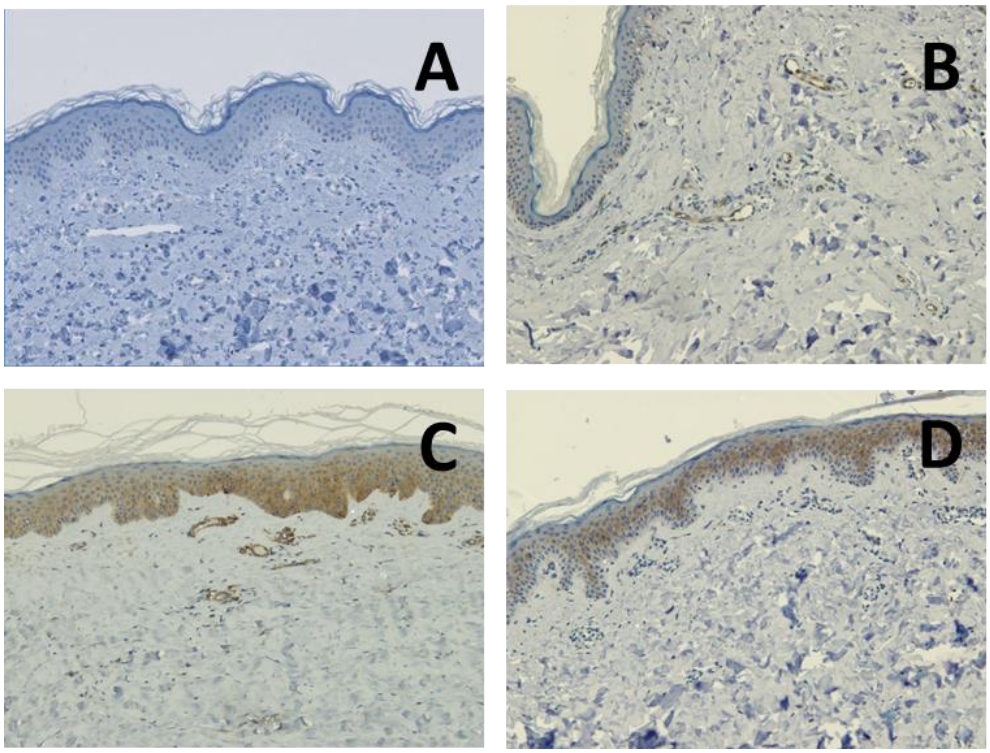

Figure 6. Histological aspects and scoring criteria of MxA stained skin biopsies. A) healthy control. **B)** endothelium scored +. **C)** epidermis and endothelium scored +. **D)** epidermis scored ++.

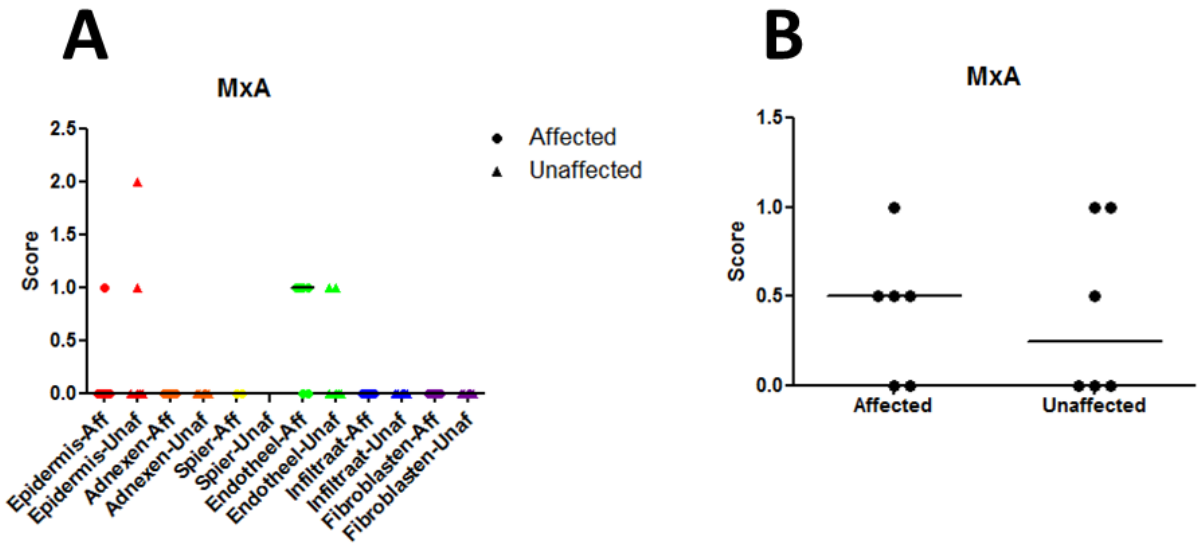

Figure 7. A) MxA expression in different skin components in affected and unaffected skin of systemic sclerosis patients. Line at median. **B)** median score of MxA expression in the epidermis and endothelium of affected versus unaffected skin of systemic sclerosis patients (n=6).

Fibroblasts Staining

Fibroblasts were stained both with immunofluorescence as with immunohistochemistry. Unfortunately, the immunofluorescence experiment is not optimalized yet, whereby results could not be analysed. So the following results and conclusions are solely drawn by the immunohistochemical staining of the fibroblasts.

The cultured fibroblasts were stimulated with high doses AGE-BSA and TGF-β1. Afterwards they were stained for the myofibroblast marker α-SMA. Expression of α-SMA shows a similar staining pattern for the different treatments, which is in and around the nucleus in all cells (*figure 9A, B, C, D*). The unstimulated cells were already positive for the α-SMA marker (*figure* 9A). Because the unstimulated cells remain fibroblasts, they should not express α-SMA, indicating this staining is not optimally performed yet. Perhaps the incubation time overnight was too long or other materials should be used. TGF-β1 is the positive control for fibroblast to myofibroblast conversion, so we expected a high α-SMA expression after this stimulation which was not found. The α-SMA expression seems to be even slightly decreased compared to the unstimulated cells (*figure 9B*). When we compare the α-SMA expression after stimulation with AGE-BSA and BSA, the AGE-BSA treated cells seems to have a higher expression, but the differences are hard to see and really small (*figure 9C, D*). To get proper results of α-SMA expression on fibroblasts after stimulation, the method of this experiment needs to be adapted until the negative control is negative and the positive control is positive for α-SMA.

Cultured cells were also stained with two different fibroblasts antigens. Surprisingly, those two antigens are showing totally different expression patterns. The 5B5 clone shows intense staining in the nucleus and very minimal staining throughout the body of the cell (*figure 9E*). The AS02 clone shows again a strong staining in the nucleus and also a strong staining in the whole body of the cells (*figure 9F*). For the 5B5 as well as the AS02 stained cells, all cells in the well showed a similar staining pattern.

Discussion

The pathogenesis of SSc is still unknown. The main problem in this disease is fibrosis in the skin and internal organs, which is responsible for morbidity and mortality in the major part of the patient population.

In this study we tried to simulate fibrosis formation in healthy dermal fibroblast by stimulating them with AGE-BSA and HMGB1. After stimulation, no upregulation of α-SMA RNA was found, indicating that no myofibroblasts were formed. Surprisingly, even after stimulation with TGF-β1 the myofibroblast marker was not increased, while this compound is known to stimulate fibroblast to myofibroblast conversion and was used as a positive control[10]. Possibly either the α-SMA primer, or the TGF-β1 stimulatory agent we used did not work properly. Another option is that the conversion to myofibroblasts did not take place. α-SMA staining of cells were done to visualize what happens to the cells. Unfortunately, we can't conclude much on behave of this experiment. We were hoping to see some cells start expressing α-SMA, while the fibroblast markers should decrease. We know from the study of Serban et al. that the differences in RNA expression levels in fibroblasts after stimulation with AGEs can be really small[45]. On the other hand, Wang et al. showed in a lung fibroblast cell line an upregulation of α-SMA mRNA after stimulation with both HMGB1 and TGF-β1. Already after 12 hours of stimulation with HMGB1 a significant higher α-SMA expression was measured in the lung fibroblasts compared to the cells at time point zero[37].

Currently, there is many evidence for a role of IFN type 1 in the pathogenesis of SSc. For example an increased expression and activation of IFN-regulated genes, also known as the IFN signature, has been found in skin biopsies and peripheral blood samples of SSc patients[39]. Also, the calculated IFN score was significantly increased in SSc patients of several stages of the disease, compared to healthy controls[40]. Since the expression of interferon inducible genes is not normally distributed, IFN scores are often calculated by log transforming of the IFN expression values and using $mean_{HC}$ and SD_{HC} to standardise expression levels. The precise formula for calculation of the IFN score is described in a SLE

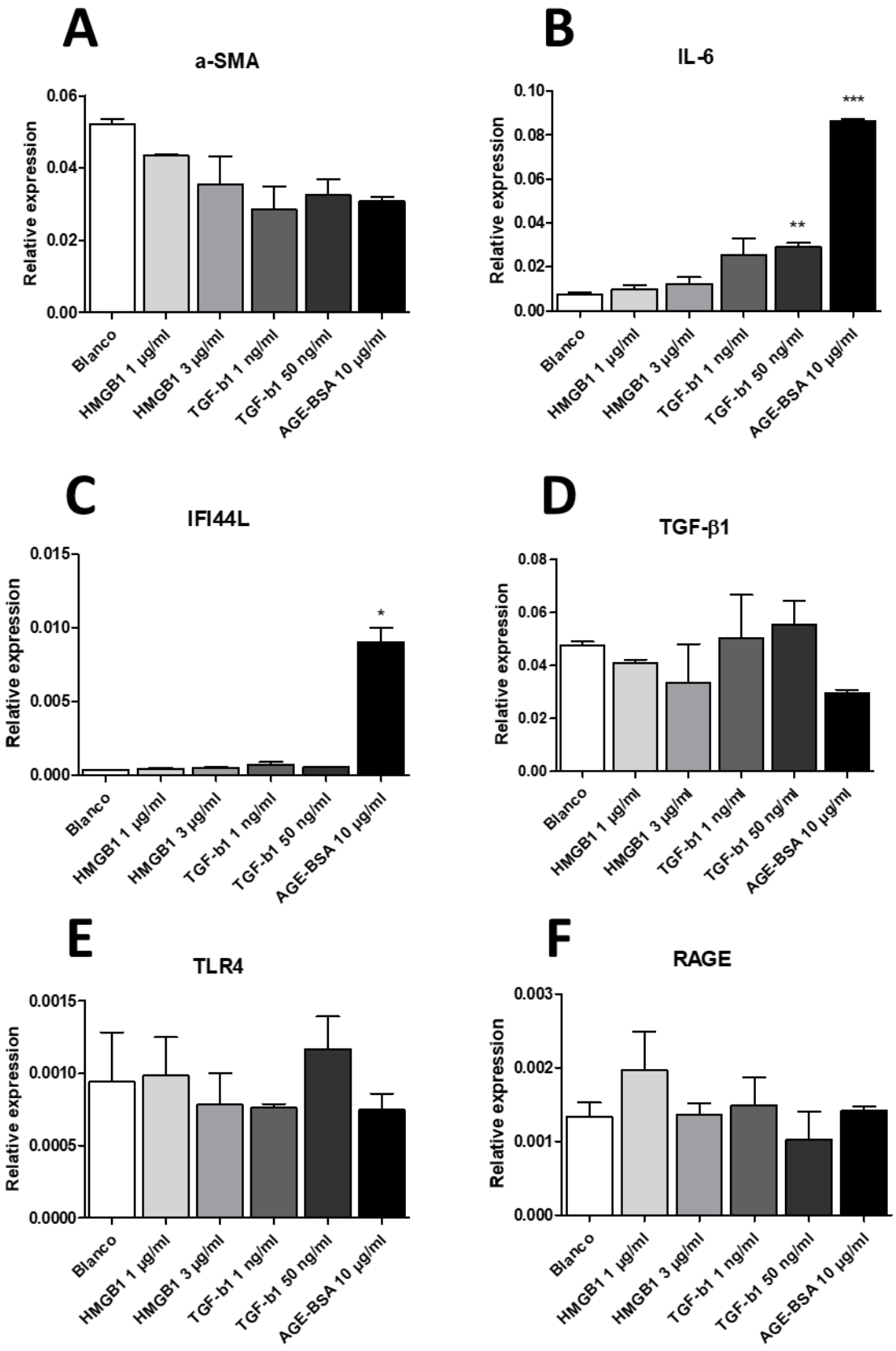

Figure 8. Human dermal fibroblasts were incubated with HMGB1, TGF-β1 or AGE-BSA at several concentrations (n=2). mRNA expression levels were measured with RT-qPCR following 24 hours of stimulation. **A)** α-smooth muscle actin. **B)** interleukin-6. ** p<0.01; *** p<0.001. **C)** interferon induced protein 44 ligand. * p<0.05 vs blanco. **D)** transforming growth factor β1. **E)** toll like receptor 4. **F)** receptor for advanced glycation end products.

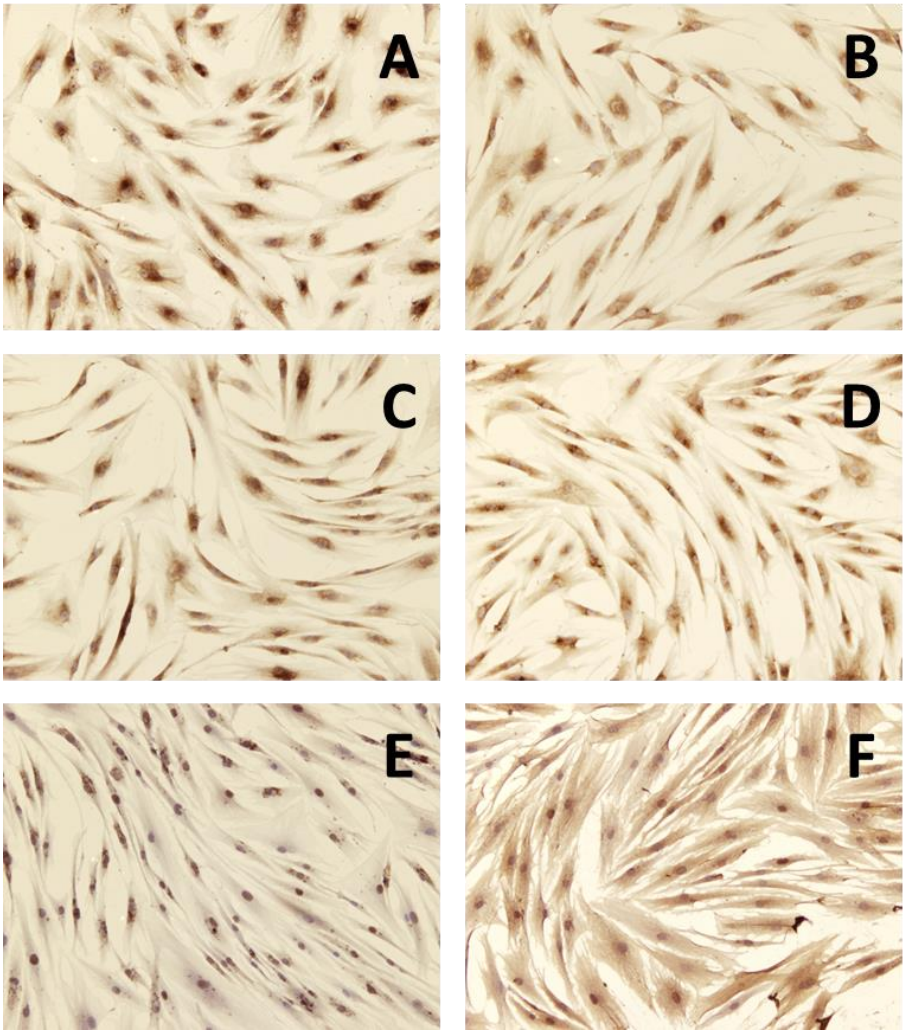

Figure 9. Immunohistochemical staining of stimulated and unstimulated human dermal fibroblasts. **A, B, C, D)** α-smooth muscle actin staining. **E)** fibroblast staining, clone 5B5. **F)** fibroblast staining, clone AS02. **A, E, F)** unstimulated. **B**) 24 hours stimulation with TGF-β1 50 ng/ml. **C)** 24 hours stimulation with AGE-BSA 100 µg/ml. **D)** 24 hours of stimulation with BSA 100 µg/ml.

study of Kirou et al[46]. Even in the earlies phases of the disease, before overt skin fibrosis an increase IFN 1 signature was observed[40]. The IFN-α induced protein MxA is considered to be a reliable marker for IFN type 1 activity[47]. Taking this all together, we expected an upregulation of MxA in the skin biopsies of the SSc patients. We found only a slight upregulation of MxA in our skin biopsies. Notably, the expression was solely found in the epidermal layer of the skin and in the epithelial cells.

An old study on Mxa expression in skin biopsies of several autoimmune diseases found a MxA expression in systemic lupus erythematosus (SLE), both in the epidermis and in infiltrate cells. A moderate MxA skin expression was found in psoriasis, lichen planus and vasculitis. Remarkably, no MxA expression was seen in SSc skin biopsies[48]. Later, many studies are performed on MxA expression in several skin conditions like vitiligo[49], morphea lesions[50], alopecia areata[51], and cutaneous lupus erythematosus (CLE)[52]. In general, MxA expression is seen in the epidermis and in the dermis, associated with inflammatory infiltrates. The morphea lesion-study found a minimal MxA expression in non-lesional skin, whereas the vitiligo study observed a strong expression in the perilesional skin[49,50]. We did not observe an association between MxA expression and T-cell infiltrates in our SSc skin

biopsies. Furthermore the MxA expression pattern in our biopsies was similar in affected and unaffected SSc skin.

In our HDF stimulation experiment, we discovered a significant increase of IFN type 1 marker IFI44L mRNA in the HDFs after stimulation with AGE-BSA. Although no effect of IFI44L mRNA expression levels was observed after HMGB1 and TGF-β1 treatment. The effects of IFN type 1 is mostly studied in monocytes, but some pro-fibrotic proteins which are found in monocytes, are also produced by fibroblasts, partially in response to TLR4 binding[53], indicating that also fibroblasts can induce a pro-fibrotic milieu as a response of IFN type 1.

The TLR receptor family is suggested to play a key role in fibroblast activation via the innate immune system in the context of SSc[54]. Many DAMPs are known to be an endogenous ligand for TLR4, among which HMGB1[55,56]. A previous study revealed that TLR4 colocalized strongly with myofibroblasts in lung biopsies of SSc patients[57]. In addition, it is known that TLR4 and certain endogenous TLR ligands are elevated in skin and lung tissues from SSc patients and this levels correlate with clinical disease parameters[56]. The mRNA levels of TLR4 were not increased in our skin fibroblasts after different treatments, including a high dose of HMGB1 treatment.

The most important receptor in this study is RAGE, to which HMGB1 and AGEs can bind to induce inflammatory reactions, and pro-survival responses[58]. Just like TLR4, we did not observe an upregulation of RAGE mRNA in the HDFs in response to the treatments. Unfortunately, the immunohistochemical staining of RAGE in the SSc skin biopsies was not clarifying, because we were not sure how to interpret them. We explored a strong straining throughout the complete biopsy, which might be a false positive signal.
Formerly, RAGE was thought to be solely membrane bound, because it is a transmembrane receptor, but now we know a splice variant of RAGE (endogenous secretory RAGE or esRAGE) as well as soluble RAGE (sRAGE) can get enzymatically cleaved from the membrane bound variant of RAGE[59,60]. As a result, in addition to expression in tissue, sRAGE can also be measured in serum. Previous results have shown elevated sRAGE levels in the serum of SSc patients. Furthermore this increase is correlated to severity of skin and pulmonary fibrosis, and many other organ involvements. Notably, sRAGE levels of SSc patients could not be correlated with TNF-α or IL-6 cytokine levels[30]. Perhaps, our immunohistochemical RAGE staining was not clarifying, because not solely membrane bound RAGE, but also sRAGE was targeted by our antibody. In future research we should use separate antibodies for both membrane bound RAGE and sRAGE to clarify this hypothesis.
An interesting note is that Iwamura et al. did not find a significant correlation between total RAGE protein levels in biopsies and gene expression levels measured by PCR[58], indicating that those different experiments can't be interchanged or compared. Logically mRNA levels increased previous to an increase in protein levels.

The main ligands of RAGE are AGEs and HMGB1. Whereas HMGB1 is well known to be also ligand for TLR4, this is not clarified yet for AGEs.
We are the first to demonstrate an upregulation of MG-H1 in the skin of SSc patients, independent whether the skin is affected or not. This indicates SSc is truly a systemic disorder with involvement of the skin, rather than just a diseased skin. Previous research demonstrates that MG-H1 is the major AGE which is found in tissues and body fluids in many circumstances, for example diabetes (including an association with (vascular) complications), renal failure and aging. Even a critical role in renal failure disease mechanism is suggested, because they could relate MG-H1 accumulation to disease progression and quality of therapeutic intervention[24]. Several other studies confirm that serum levels of AGEs are related to disease progression and complications in diabetes[61-63]. Genuth et al. confess AGEs expression in the skin, especially CML is significantly associated with progression of diabetic microvascular complications[64]. Another study showed that blocking of AGE precursor glyoxalase 1 (GLO1) protects against diabetic retinopathy is also strongly linked to AGE formation and cell damage[65].

The relation between AGEs and diabetes mellitus is becoming increasingly clear, although this has still to be discovered in SSc. Against our expectation, the expression of CML and pentosidine were not increased in our SSc skin biopsies. In the context of SSc, previous studies showed an upregulation of CML in skin biopsies[28], as well as in serum[66]. We did observe colocalization of CML with elastin fibers in SSc skin biopsies. Previously it is shown that extracellular matrix constituent elastin production is increased in SSc skin[67,68]. On the other hand, also the breakdown products of elastin are increased in SSc[69,70]. In contrast to what we found, colocalization of CML with fibroblasts and endothelial cells is reported previously[44].
We found no difference in pentosidine expression in the SSc skin biopsies compared to healthy control skin. Just like the other AGEs we discussed, also increased serum pentosidine is associated with diabetic complications, especially with microvascular injury. The same study found an influence of age on pentosidine serum levels, namely increasing pentosidine levels were associated with older age[71]. In contrast, the same author indicated no influence of age on the pentosidine serum levels in the context of multiple sclerosis[72]. In general, increased AGEs are associated with age, even in healthy persons[73]. This could be a possible confounder for the expression of AGEs in our skin biopsies. Unfortunately, we don't have access to the characteristics of the healthy control, due to privacy considerations of patient information. It is well known that pentosidine is higher expressed in sun exposed skin[74]. As some of our skin samples are also sun exposed, we would expect to discover some expression of pentosidine in our patients. Another possibility is that pentosidine does not contribute to the pathogenesis of SSc. In future experiments, we need to include diabetes skin as a positive control for CML and pentosidine expression. Hereby we can hopefully conclude that our antibodies are working properly.
The final ligand we will describe in this report is HMGB1. It was expected to find increased HMGB1 activation in our SSc skin biopsies. On the one hand, the role of HMGB1 in SSc is not clear yet, although Yoshizaki et al. showed already increased serum HMGB1 levels in SSc patients compared to healthy controls almost ten years ago[30]. It is clearly reported that HMGB1 upregulation stimulates the onset of fibrosis by increasing the TGF-β1 production of fibroblasts[37,38]. ROS increases HMGB1 activation which possibly contributes to the microvascular injury of patients with SSc[75].

Taking all this together, MG-H1 is the most prominent AGE in affected, as well as in unaffected SSc skin, indicating the effects of MG-H1 are systemic and not restricted to the skin. Bhattacharyya et al. already suggested this in 2011: "Because the skin is a prominent organ affected in SSc and is readily accessible for biopsy, much of the recently described information regarding fibrosis relates to skin cells. However, it is reasonable to presume that the pathways and mechanisms implicated in skin fibrosis are also operational in other cell types and organs"[18]. Presumably, the effects of MG-H1 goes via binding to RAGE, but we could not demonstrate this. To clarify this, we should use a RAGE blocker together with a MG-H1 antibody in a follow-up study. The results of our fibroblast stimulation experiments did not match our expectations. It seems that the fibroblasts did not convert to myofibroblasts. Although the inflammatory markers showed an upregulation after AGE-BSA stimulation, the receptors RAGE and TLR4 did not. So I think an inflammatory milieu was created, by upregulation of IL-6 and IFI44L, and it will take more time to develop ROS and induce fibrosis. It is known that ROS can be induced via many growth factors and cytokines, including IL-6 and TGF-β1[76], but since the TGF-β1 mRNA levels were not increased, this is not happened (yet) in our HDFs. It would be very interesting to isolate fibroblasts from SSc patients in future research and investigate how they respond on stimulation. Furthermore, previous studies suggest ROS is created by endothelial cell damage as a reaction to ischemia[10,18]. Another possibility is that, next to TGF-β1, also other triggers could also be important for myofibroblast differentiation, which were perhaps not present in our cells, such as Wnt ligands, Hedgehog, Jagged-Notch signalling, and bioactive ligands, for example peroxisome proliferator-activated receptor γ (PPAR-γ)[18].

In conclusion, MG-H1 proteins are upregulated in both affected and unaffected SSc skin, indicating it has a role in the pathogenesis of SSc. AGE-BSA stimulation in healthy HDFs did not result in fibrosis,

but an inflammatory milieu was created, suggesting a pre-fibrotic stadium. To clarify how fibrosis arises in SSc, future research is necessary.

Bibliography

1. Gabrielli A, Avvedimento EV, Krieg T. Scleroderma. *N Engl J Med*. 2009;360(19):1989-2003.

2. Stern EP, Denton CP. The pathogenesis of systemic sclerosis. *Rheum Dis Clin North Am*. 2015;41(3):367-382.

3. Rongioletti F, Kaiser F, Cinotti E, et al. Scleredema. A multicentre study of characteristics, comorbidities, course and therapy in 44 patients. *J Eur Acad Dermatol Venereol*. 2015;29(12):2399-2404.

4. Li L, Zuo X, Luo H, et al. Mortality trend of inpatients with connective tissue diseases: 2005-2014. *Zhong Nan Da Xue Xue Bao Yi Xue Ban*. 2017;42(8):927-933.

5. Chifflot H, Fautrel B, Sordet C, Chatelus E, Sibilia J. Incidence and prevalence of systemic sclerosis: A systematic literature review. *Semin Arthritis Rheum*. 2008;37(4):223-235.

6. LeRoy EC, Black C, Fleischmajer R, et al. Scleroderma (systemic sclerosis): Classification, subsets and pathogenesis. *J Rheumatol*. 1988;15(2):202-205.

7. Romanowska-Prochnicka K, Walczyk M, Olesinska M. Recognizing systemic sclerosis: Comparative analysis of various sets of classification criteria. *Reumatologia*. 2016;54(6):296-305.

8. Pattanaik D, Brown M, Postlethwaite BC, Postlethwaite AE. Pathogenesis of systemic sclerosis. *Front Immunol*. 2015;6:272.

9. Kuwana M. Circulating anti-nuclear antibodies in systemic sclerosis: Utility in diagnosis and disease subsetting. *J Nippon Med Sch*. 2017;84(2):56-63.

10. Varga J, Abraham D. Systemic sclerosis: A prototypic multisystem fibrotic disorder. *J Clin Invest*. 2007;117(3):557-567.

11. Desmouliere A, Geinoz A, Gabbiani F, Gabbiani G. Transforming growth factor-beta 1 induces alpha-smooth muscle actin expression in granulation tissue myofibroblasts and in quiescent and growing cultured fibroblasts. *J Cell Biol*. 1993;122(1):103-111.

12. Ihn H. Scleroderma, fibroblasts, signaling, and excessive extracellular matrix. *Curr Rheumatol Rep*. 2005;7(2):156-162.

13. Ihn H. Autocrine TGF-beta signaling in the pathogenesis of systemic sclerosis. *J Dermatol Sci*. 2008;49(2):103-113.

14. Schulz JN, Plomann M, Sengle G, Gullberg D, Krieg T, Eckes B. New developments on skin fibrosis - essential signals emanating from the extracellular matrix for the control of myofibroblasts. *Matrix Biol*. 2018.

15. Leroy EC. Connective tissue synthesis by scleroderma skin fibroblasts in cell culture. *J Exp Med*. 1972;135(6):1351-1362.

16. LeRoy EC. Increased collagen synthesis by scleroderma skin fibroblasts in vitro: A possible defect in the regulation or activation of the scleroderma fibroblast. *J Clin Invest*. 1974;54(4):880-889.

17. Wei J, Bhattacharyya S, Tourtellotte WG, Varga J. Fibrosis in systemic sclerosis: Emerging concepts and implications for targeted therapy. *Autoimmun Rev*. 2011;10(5):267-275.

18. Bhattacharyya S, Wei J, Varga J. Understanding fibrosis in systemic sclerosis: Shifting paradigms, emerging opportunities. *Nat Rev Rheumatol*. 2011;8(1):42-54.

19. Raj DS, Choudhury D, Welbourne TC, Levi M. Advanced glycation end products: A nephrologist's perspective. *Am J Kidney Dis*. 2000;35(3):365-380.

20. Goldin A, Beckman JA, Schmidt AM, Creager MA. Advanced glycation end products: Sparking the development of diabetic vascular injury. *Circulation*. 2006;114(6):597-605.

21. Dyer DG, Dunn JA, Thorpe SR, et al. Accumulation of maillard reaction products in skin collagen in diabetes and aging. *J Clin Invest*. 1993;91(6):2463-2469.

22. Singh R, Barden A, Mori T, Beilin L. Advanced glycation end-products: A review. *Diabetologia*. 2001;44(2):129-146.

23. John WG, Lamb EJ. The maillard or browning reaction in diabetes. *Eye (Lond)*. 1993;7 (Pt 2)(Pt 2):230-237.

24. Rabbani N, Thornalley PJ. Methylglyoxal, glyoxalase 1 and the dicarbonyl proteome. *Amino Acids*. 2012;42(4):1133-1142.

25. Ramasamy R, Vannucci SJ, Yan SS, Herold K, Yan SF, Schmidt AM. Advanced glycation end products and RAGE: A common thread in aging, diabetes, neurodegeneration, and inflammation. *Glycobiology*. 2005;15(7):16R-28R.

26. Brownlee M. Advanced protein glycosylation in diabetes and aging. *Annu Rev Med*. 1995;46:223-234.

27. de Vos LC, Lefrandt JD, Dullaart RP, Zeebregts CJ, Smit AJ. Advanced glycation end products: An emerging biomarker for adverse outcome in patients with peripheral artery disease. *Atherosclerosis*. 2016;254:291-299.

28. Davies CA, Herrick AL, Cordingley L, Freemont AJ, Jeziorska M. Expression of advanced glycation end products and their receptor in skin from patients with systemic sclerosis with and without calcinosis. *Rheumatology (Oxford)*. 2009;48(8):876-882.

29. Hudson BI, Lippman ME. Targeting RAGE signaling in inflammatory disease. *Annu Rev Med*. 2018;69:349-364.

30. Yoshizaki A, Komura K, Iwata Y, et al. Clinical significance of serum HMGB-1 and sRAGE levels in systemic sclerosis: Association with disease severity. *J Clin Immunol*. 2009;29(2):180-189.

31. Xie J, Mendez JD, Mendez-Valenzuela V, Aguilar-Hernandez MM. Cellular signalling of the receptor for advanced glycation end products (RAGE). *Cell Signal*. 2013;25(11):2185-2197.

32. Dadoniene J, Cypiene A, Ryliskyte L, Rugiene R, Ryliskiene K, Laucevicius A. Skin autofluorescence in systemic sclerosis is related to the disease and vascular damage: A cross-sectional analytic study of comparative groups. *Dis Markers*. 2015;2015:837470.

33. Andersson U, Tracey KJ. HMGB1 is a therapeutic target for sterile inflammation and infection. *Annu Rev Immunol*. 2011;29:139-162.

34. Andersson U, Wang H, Palmblad K, et al. High mobility group 1 protein (HMG-1) stimulates proinflammatory cytokine synthesis in human monocytes. *J Exp Med*. 2000;192(4):565-570.

35. Youn JH, Oh YJ, Kim ES, Choi JE, Shin JS. High mobility group box 1 protein binding to lipopolysaccharide facilitates transfer of lipopolysaccharide to CD14 and enhances lipopolysaccharide-mediated TNF-alpha production in human monocytes. *J Immunol*. 2008;180(7):5067-5074.

36. Maugeri N, Franchini S, Campana L, et al. Circulating platelets as a source of the damage-associated molecular pattern HMGB1 in patients with systemic sclerosis. *Autoimmunity*. 2012;45(8):584-587.

37. Wang Q, Wang J, Wang J, et al. HMGB1 induces lung fibroblast to myofibroblast differentiation through NFkappaBmediated TGFbeta1 release. *Mol Med Rep*. 2017;15(5):3062-3068.

38. Ebina M, Taniguchi H, Miyasho T, et al. Gradual increase of high mobility group protein b1 in the lungs after the onset of acute exacerbation of idiopathic pulmonary fibrosis. *Pulm Med*. 2011;2011:916486.

39. Wu M, Assassi S. The role of type 1 interferon in systemic sclerosis. *Front Immunol*. 2013;4:266.

40. Brkic Z, van Bon L, Cossu M, et al. The interferon type I signature is present in systemic sclerosis before overt fibrosis and might contribute to its pathogenesis through high BAFF gene expression and high collagen synthesis. *Ann Rheum Dis*. 2016;75(8):1567-1573.

41. Higgs BW, Liu Z, White B, et al. Patients with systemic lupus erythematosus, myositis, rheumatoid arthritis and scleroderma share activation of a common type I interferon pathway. *Ann Rheum Dis*. 2011;70(11):2029-2036.

42. Haller O, Kochs G. Human MxA protein: An interferon-induced dynamin-like GTPase with broad antiviral activity. *J Interferon Cytokine Res*. 2011;31(1):79-87.

43. van den Hoogen F, Khanna D, Fransen J, et al. 2013 classification criteria for systemic sclerosis: An american college of rheumatology/european league against rheumatism collaborative initiative. *Arthritis Rheum*. 2013;65(11):2737-2747.

44. Crisan M, Taulescu M, Crisan D, et al. Expression of advanced glycation end-products on sun-exposed and non-exposed cutaneous sites during the ageing process in humans. *PLoS One*. 2013;8(10):e75003.

45. Serban AI, Stanca L, Geicu OI, Munteanu MC, Dinischiotu A. RAGE and TGF-beta1 cross-talk regulate extracellular matrix turnover and cytokine synthesis in AGEs exposed fibroblast cells. *PLoS One*. 2016;11(3):e0152376.

46. Kirou KA, Lee C, George S, et al. Coordinate overexpression of interferon-alpha-induced genes in systemic lupus erythematosus. *Arthritis Rheum*. 2004;50(12):3958-3967.

47. Airo P, Ghidini C, Zanotti C, et al. Upregulation of myxovirus-resistance protein A: A possible marker of type I interferon induction in systemic sclerosis. *J Rheumatol*. 2008;35(11):2192-2200.

48. Fah J, Pavlovic J, Burg G. Expression of MxA protein in inflammatory dermatoses. *J Histochem Cytochem*. 1995;43(1):47-52.

49. Bertolotti A, Boniface K, Vergier B, et al. Type I interferon signature in the initiation of the immune response in vitiligo. *Pigment Cell Melanoma Res*. 2014;27(3):398-407.

50. Ghoreishi M, Vera Kellet C, Dutz JP. Type 1 IFN-induced protein MxA and plasmacytoid dendritic cells in lesions of morphea. *Exp Dermatol*. 2012;21(6):417-419.

51. Ghoreishi M, Martinka M, Dutz JP. Type 1 interferon signature in the scalp lesions of alopecia areata. *Br J Dermatol*. 2010;163(1):57-62.

52. Wenzel J, Worenkamper E, Freutel S, et al. Enhanced type I interferon signalling promotes Th1-biased inflammation in cutaneous lupus erythematosus. *J Pathol*. 2005;205(4):435-442.

53. Chizzolini C, Brembilla NC, Montanari E, Truchetet ME. Fibrosis and immune dysregulation in systemic sclerosis. *Autoimmun Rev*. 2011;10(5):276-281.

54. Sakoguchi A, Nakayama W, Jinnin M, et al. The expression profile of the toll-like receptor family in scleroderma dermal fibroblasts. *Clin Exp Rheumatol*. 2014;32(6 Suppl 86):S-4-9.

55. Salem A, Almahmoudi R, Vehvilainen M, Salo T. Role of the high mobility group box 1 signalling axes via the receptor for advanced glycation end-products and toll-like receptor-4 in the immunopathology of oral lichen planus: A potential drug target? *Eur J Oral Sci*. 2018;126(3):244-248.

56. Bhattacharyya S, Midwood KS, Yin H, Varga J. Toll-like receptor-4 signaling drives persistent fibroblast activation and prevents fibrosis resolution in scleroderma. *Adv Wound Care (New Rochelle)*. 2017;6(10):356-369.

57. Bhattacharyya S, Kelley K, Melichian DS, et al. Toll-like receptor 4 signaling augments transforming growth factor-beta responses: A novel mechanism for maintaining and amplifying fibrosis in scleroderma. *Am J Pathol*. 2013;182(1):192-205.

58. Iwamura M, Yamamoto Y, Kitayama Y, et al. Epidermal expression of receptor for advanced glycation end products (RAGE) is related to inflammation and apoptosis in human skin. *Exp Dermatol*. 2016;25(3):235-237.

59. Cheng C, Tsuneyama K, Kominami R, et al. Expression profiling of endogenous secretory receptor for advanced glycation end products in human organs. *Mod Pathol*. 2005;18(10):1385-1396.

60. Yonekura H, Yamamoto Y, Sakurai S, et al. Novel splice variants of the receptor for advanced glycation end-products expressed in human vascular endothelial cells and pericytes, and their putative roles in diabetes-induced vascular injury. *Biochem J*. 2003;370(Pt 3):1097-1109.

61. Fosmark DS, Torjesen PA, Kilhovd BK, et al. Increased serum levels of the specific advanced glycation end product methylglyoxal-derived hydroimidazolone are associated with retinopathy in patients with type 2 diabetes mellitus. *Metabolism*. 2006;55(2):232-236.

62. Yamaguchi M, Nakamura N, Nakano K, et al. Immunochemical quantification of crossline as a fluorescent advanced glycation endproduct in erythrocyte membrane proteins from diabetic patients with or without retinopathy. *Diabet Med*. 1998;15(6):458-462.

63. van Eupen MG, Schram MT, Colhoun HM, et al. The methylglyoxal-derived AGE tetrahydropyrimidine is increased in plasma of individuals with type 1 diabetes mellitus and in atherosclerotic lesions and is associated with sVCAM-1. *Diabetologia*. 2013;56(8):1845-1855.

64. Genuth S, Sun W, Cleary P, et al. Glycation and carboxymethyllysine levels in skin collagen predict the risk of future 10-year progression of diabetic retinopathy and nephropathy in the diabetes control and complications trial and epidemiology of diabetes interventions and complications participants with type 1 diabetes. *Diabetes*. 2005;54(11):3103-3111.

65. Berner AK, Brouwers O, Pringle R, et al. Protection against methylglyoxal-derived AGEs by regulation of glyoxalase 1 prevents retinal neuroglial and vasodegenerative pathology. *Diabetologia*. 2012;55(3):845-854.

66. Kaloudi O, Basta G, Perfetto F, et al. Circulating levels of nepsilon-(carboxymethyl)lysine are increased in systemic sclerosis. *Rheumatology (Oxford)*. 2007;46(3):412-416.

67. Quaglino D,Jr, Bergamini G, Boraldi F, Manzini E, Davidson JM, Pasquali Ronchetti I. Connective tissue in skin biopsies from patients suffering systemic sclerosis. *J Submicrosc Cytol Pathol*. 1996;28(2):287-296.

68. Pasquali Ronchetti I, Guerra D, Quaglino D,Jr, et al. Dermal elastin and collagen in systemic sclerosis. effect of D-penicillamine treatment. *Clin Exp Rheumatol*. 1989;7(4):373-383.

69. Davis EC, Blattel SA, Mecham RP. Remodeling of elastic fiber components in scleroderma skin. *Connect Tissue Res*. 1999;40(2):113-121.

70. Hong YJ, Kim J, Oh BR, et al. Serum elastin-derived peptides and anti-elastin antibody in patients with systemic sclerosis. *J Korean Med Sci*. 2012;27(5):484-488.

71. Sternberg M, M'bemba J, Urios P, et al. Skin collagen pentosidine and fluorescence in diabetes were predictors of retinopathy progression and creatininemia increase already 6years after punch-biopsy. *Clin Biochem*. 2016;49(3):225-231.

72. Sternberg Z, Hennies C, Sternberg D, et al. Plasma pentosidine: A potential biomarker in the management of multiple sclerosis. *Mult Scler*. 2011;17(2):157-163.

73. Prasad C, Imrhan V, Marotta F, Juma S, Vijayagopal P. Lifestyle and advanced glycation end products (AGEs) burden: Its relevance to healthy aging. *Aging Dis*. 2014;5(3):212-217.

74. Beisswenger PJ, Howell S, Mackenzie T, Corstjens H, Muizzuddin N, Matsui MS. Two fluorescent wavelengths, 440(ex)/520(em) nm and 370(ex)/440(em) nm, reflect advanced glycation and oxidation end products in human skin without diabetes. *Diabetes Technol Ther*. 2012;14(3):285-292.

75. Maugeri N, Rovere-Querini P, Baldini M, et al. Oxidative stress elicits platelet/leukocyte inflammatory interactions via HMGB1: A candidate for microvessel injury in sytemic sclerosis. *Antioxid Redox Signal*. 2014;20(7):1060-1074.

76. Vona R, Giovannetti A, Gambardella L, Malorni W, Pietraforte D, Straface E. Oxidative stress in the pathogenesis of systemic scleroderma: An overview. *J Cell Mol Med*. 2018.

Protocols

Immunohistochemistry skin biopsies

- Deparaffinise: xylene (2x 10 min), 100% ethanol (2x 5 min), 96% ethanol (2x 5 min), 70% ethanol (2x 5 min) and demi water (1x 5 min)
- Antigen retrieval: 60 min in 10 µM Tris HCl pH 9 or sodiumcitrate buffer pH 6 in water bath at 90 °C
- 30 minute cooldown to room temperature
- 3x wash in PBS (3x 5 min) on shaker
- Endogenous peroxidase blocking: 0.3% H_2O_2 in PBS (30 minutes at RT)
- 3x wash in PBS (3x 5 min) on shaker
- Incubation primary antibody overnight at 4 °C in PBS 1% BSA; apply 50 µl per skin biopsy
- 3x wash in PBS (2x 5 min, 1x 30 min) on shaker
- Incubation secondary antibody for 1 hour at RT in PBS 1% BSA; apply 50 µl per skin biopsy
- 3x wash in PBS (3x 5 min) on shaker
- Apply DAB straining with kit (DAKO K4006), 1 ml buffersubstrate with 1 drop (20 µl) DAB + Chromogen for 10 min at RT
- 3x wash in PBS (3x 5 min) on shaker
- Haematoxilin staining for 5 seconds
- Wash under tab water for 10 minutes
- Cover with Kaisers glycerin and glass

Passage cells

- Work sterile!
- Heat medium and sterile PBS at 37 °C
- Defreeze 3 ml trypsin (can defreeze maximum three times)
- Store 7 ml medium in a 15 ml tube
- Remove the residual medium
- Wash 3x with 3 ml sterile PBS
- Add 3 ml 0.05% trypsin to the plate
- Incubate 5 minutes in the incubator at 37 °C
- Check under the microscope whether the cells are released from the bottom of the flask
- Add the 7 ml stored medium to the plate and mix with trypsin, this stops the reaction of trypsin
- Remove all the fluid from the flask and put in a 15 ml tube
- Wash the plate 1x with sterile PBS and add PBS to the tube
- Check under the microscope whether the flask is empty
- Centrifuge tube:
    - 330 rcf
    - 8 min
    - 20 °C
- The cells are at the bottom of the tube now. Carefully remove the medium
- Add new medium to the cells and mix the pellet
- Add approximately 750.000 cells per 75 cm^2 culture flasks in 10-15 ml medium
- Put flasks in the incubator at 37 °C with the lit a bit loose

RNA isolation

- Discard supernatant from cells, wash with PBS, and add 1 ml Trizol to each well
- Incubate 5 min at RT with Trizol and put each sample in a separate tube
- Check whether the plate is empty with the microscope

- Either directly perform RNA isolation or store samples at -80 °C
- When applicable, take samples from -80 °C freezer and completely thaw samples
- Add 200 µl chloroform to all tubes
- Vortex samples for at least 15 seconds and incubate for 2-3 minutes at RT
- Centrifuge tubes for 15 minutes at 4 °C and 10000 rpm
- Collect clear/aqueous upper layer (approximately 460 µl) in new tubes
- Add 500 µl isopropanol to each tube and vortex samples
- Incubate samples for at least 10 minutes at RT
- Centrifuge tubes for 10 minutes at 4 °C and 10000 rpm
- Decant supernatant, add 1 ml ice-cold 75% ethanol and vortex briefly
- Centrifuge tubes for 5 minutes at 4 °C and 8000 rpm
- Decant ethanol and put tubes upside down to dry pellets (approximately 1 hour)

DNAse treatment

- Prepare for n+1 samples a mixture of 22.5 µl RNAse-free water, 2.5 µl DNAse buffer and 1 µl DNAse
- Add 26 µl to each sample and resuspend pellet
- Briefly centrifuge tubes to ensure all fluid is on the bottom of the tube and put tubes in 37˚C incubator for 30 minutes
- Resuspend inactivation mixture by vortexing it and add 5 µl inactivation reagent to all samples, resuspend and centrifuge briefly
- RNA is present in the supernatant and cDNA can be synthesized according to protocol 'cDNA synthesis'
- Keep samples on ice from here onwards

cDNA synthesis

- Measure RNA concentrations in samples
    - RNA concentration $\leq$ 100 ng/µl use all (= 25 µl) RNA and put in small PCR tubes
    - RNA concentration $\geq$ 100 ng/ µl calculate how much you need and put in small PCR tubes
        - RNA needed (µl) = 2500 / (RNA concentration in sample)
- Heat samples for 10 minutes at 65 °C in water bath, afterwards keep samples on ice until PCR reaction is performed
- Prepare mix per sample (+1 extra):
    - 1 µl 25 mM dNTP's
    - 1 µl M-MLV RT enzyme
    - 5 µl 5x First Strand buffer
    - 0.9 µl 0.1M DTT
    - 0.5 µl Oligo(dT)12-18 Primer
    - 6.6 µl DEPC water
- Add 15 µl mix to each tube
- Put PCR tubes in PCR machine and perform the following RT-PCR-reaction:
    1. 60 minutes 41 °C
    2. 5 minutes 95 °C
    3. ∞ 4 °C
    4. Hot start → no
- Store cDNA at -20 °C

RT-qPCR

- Apply 1 µl cDNA in duplo into a 384-well plate

- Centrifuge plate for 10 minutes under a vacuum using the DNA speedvac at a medium drying rate
- Add the desired primer per sample:
    - 0.5 µl primer/probe
    - 4.5 µl water
    - 5 µl taqman premix
- Vortex and centrifuge primer shortly, and add 10 µl to each well
- Seal plate with an Optical Seal by Applied Biosystems
- Shortly centrifuge plate to ensure all mix is on the bottom of the plate
- Put the plate in the Quanstudio 7 Flex
- Go to Quanstudio Real-Time PCR software
- Choose new experiment:
    - Setup → experiment properties → choose: Quantstudio 7 Flex System, 384- well, comperative Ct (ΔΔCt), TaqMan Reagents, standard
    - Setup → run method → Volume per well is 10 µl, delete first step, second step is 15 minutes at 95 °C
- Choose save → save as and save experiment in folder qPCR-documents
- Go to run → start run and click on the machine number

Immunofluorescence cells

- Fixate cells with 1% formaldehyde (RT) for 20 minutes 100 µl/well
- Wash 3x with PBS 300 µl/well
- Permeabilise with 0.2% Triton X-100 (RT) for 30 minutes 100 µl/well. Vortex well before use!!
- Wash 3x with PBS 300 µl/well
- Block with 2% BSA (RT) 30 minutes 100 µl/well
- Incubate with primary antibody overnight at 4 °C, dilute antibody in PBS+ (0.5% Tween, 0.5% BSA in PBS). Apply 100 µl/well
- Wash 3x with PBS+ 300 µl/well
- Incubate with DAPI in the dark, diluted in PBS+, 100 µl/well
- Wash 3x with PBS+ 300 µl/well
- Incubate with secondary antibody 30 minutes at RT in the dark, dilute in PBS+. Apply 100 µl/well
- Cover with citifluor and glass

Immunohistochemistry cells

- Fixate cells with 1% formaldehyde (RT) for 20 minutes 100 µl/well
- Wash 3x with PBS 300 µl/well
- Permeabilise with 0.2% Triton X-100 (RT) for 30 minutes 100 µl/well. Vortex well before use!!
- Wash 3x with PBS 300 µl/well
- Block with 2% BSA (RT) 30 minutes 100 µl/well
- Incubate with primary antibody overnight at 4 °C, dilute antibody in PBS 1% BSA, apply 100 µl/well
- Wash 3x with PBS 300 µl/well
- Incubate with secondary antibody for 30 minutes at RT, dilute antibody in PBS 1% BSA, apply 100 µl/well
- Wash 3x with PBS 300 µl/well
- Apply DAB straining with kit (DAKO K4006), 1 ml buffersubstrate with 1 drop (20 µl) DAB + Chromogen for 10 min at RT, 100 µl/well
- Wash 3x with PBS 300 µl/well
- Haematoxilin staining for 5 seconds

- Wash under tab water for 10 minutes
- Cover with Kaisers glycerin and glass